

## Photoluminescence of hydrophilic silicon nanocrystals in aqueous solutions

This article has been downloaded from IOPscience. Please scroll down to see the full text article.

2011 Nanotechnology 22 215704

(<http://iopscience.iop.org/0957-4484/22/21/215704>)

View [the table of contents for this issue](#), or go to the [journal homepage](#) for more

Download details:

IP Address: 193.205.206.85

The article was downloaded on 11/05/2011 at 14:33

Please note that [terms and conditions apply](#).

# Photoluminescence of hydrophilic silicon nanocrystals in aqueous solutions

Nikola Prtljaga<sup>1</sup>, Elvira D'Amato<sup>1</sup>, Alessandro Pitanti<sup>1,2</sup>,  
Romain Guider<sup>1</sup>, Elena Froner<sup>1</sup>, Silvia Larcheri<sup>1</sup>, Marina Scarpa<sup>1</sup>  
and Lorenzo Pavesi<sup>1</sup>

<sup>1</sup> Department of Physics, University of Trento, Via Sommarive 14, I-38123 Trento, Italy

<sup>2</sup> NEST, Scuola Normale Superiore, Istituto di nanoscienze—CNR, Piazza San Silvestro 12, I-56127 Pisa, Italy

E-mail: [nikolap@science.unitn.it](mailto:nikolap@science.unitn.it)

Received 27 December 2010, in final form 28 February 2011

Published 31 March 2011

Online at [stacks.iop.org/Nano/22/215704](http://stacks.iop.org/Nano/22/215704)

## Abstract

Stable aqueous solutions of undecylenic-acid-grafted silicon nanocrystals (Si-nc) were prepared. The time evolution of the photoluminescence properties of these hydrophilic silicon nanocrystals has been followed on different timescales (hours and days). On a short timescale (hours), Si-nc tend to agglomerate while the PL lineshape and intensity are stable.

Agglomeration can be reduced by using suitable surfactants. On a long timescale (days), oxidation of Si-nc occurs even in the presence of surfactants. These two observations render Si-nc very useful as a labeling agent for biosensing.

 Online supplementary data available from [stacks.iop.org/Nano/22/215704/mmedia](http://stacks.iop.org/Nano/22/215704/mmedia)

(Some figures in this article are in colour only in the electronic version)

## 1. Introduction

A number of different drawbacks for organic fluorescent dyes employed in imaging have been identified: overlap of excitation and emission bands, short lifetimes, narrow excitation spectral bands, photobleaching, etc [1, 2]. Diverse alternatives to dyes have been proposed: organic-based nanoparticles [3], carbon nanotubes [4], gold nanoparticles [5] and semiconductor quantum dots [6]. However, the need for additional molecular tagging [3], some concerns about their biodegradability [5, 7], the toxicity of their by-products [8], the phototoxicity [9] or the toxicity due to their structural properties [10] severely limit their actual use.

On the other hand, silicon is a common trace element in biological systems and is naturally absorbed and extracted by a number of different tissues [11]. This makes silicon a candidate for imaging applications from the point of view of biocompatibility [12] and biodegradability [13]. Moreover, to achieve the low detection limits needed for *in vivo* imaging, emission in the near-infrared (700–1000 nm) is preferable [1, 14]. Unfortunately, near-infrared (NIR) fluorescent dyes possess very low quantum yields [15]. Although silicon in its bulk form is a very poor light emitter, porous silicon [16] shows that nanocrystalline

silicon is an efficient NIR light emitter [17]. While quantum and exciton confinement are generally considered as responsible for the emission in Si-nc [18], the Si-nc surface rules the emission properties [19]. In fact, Si-nc lack long-term photoluminescence (PL) stability in air or aqueous solutions due to a rapid and efficient surface oxidation [20]. By appropriate Si-nc surface functionalization with organic molecules, improved stability to oxidation could be achieved [2, 20, 21]. However, the temporal evolution of PL of Si-nc in aqueous environment still lacks a complete description. This work concerns a study of the short-term stability of luminescence of functionalized Si-nc in water suspension with or without the presence of various surfactants in order to investigate physical coating as a strategy to improve stability. Special attention is given towards the understanding of processes that govern the time evolution of PL of these systems on different timescales.

## 2. Experimental section

### 2.1. PS formation

All chemicals were purchased from Sigma-Aldrich and employed without further purification. Photoluminescent

porous silicon (p-Si) layers were formed by galvanostatic anodization ( $80 \text{ mA cm}^{-2}$  for 5 min) of  $1 \text{ cm}^2$  chips of boron-doped p-type Si(100)-oriented wafers ( $10\text{--}20 \text{ } \Omega \text{ cm}$  resistivity, University Wafer) in a 1:2 v/v solution of 48% HF and absolute ethanol (Fluka).

## 2.2. Si-nc suspension preparation

A Schlenk flask containing undecylenic acid (0.7 M) in a toluene/ethanol mixture (1:1) was outgassed under argon for 30 min to remove the dissolved oxygen. One freshly prepared p-Si chip was then transferred into this Schlenk flask and sonicated in a Uniset AC2 (Emmegi) ultrasonic bath under white light (ELC bulb 250 W) irradiation for 30 min with continuous argon bubbling. An argon atmosphere was used during the whole procedure. After sonication, the silicon chip was removed and the suspension of nanoparticles was stirred for 1 h under the argon flux and illumination. After reaction, a clear solution of COOH-terminated nanoparticles was obtained. The luminescent particle suspension was filtered through a  $0.2 \text{ } \mu\text{m}$  syringe filter (Sartorius Minisart SRP25) and then the solvent was removed under reduced pressure with a Rotor-Vapor (Heidolph). The resulting material was redispersed in ethanol containing HCl (1 mM). Purification from undecylenic acid and residual solvents was performed by filtration cycles over Vivaspin 15 concentrators (Sartorius) with a molecular weight cutoff (MWCO) of 100 000. The retentate was collected after each cycle and the filter was rinsed with pure ethanol + 1 mM HCl. This process was repeated five times. As a result, an ethanol suspension of concentrated COOH-terminated silicon nanocrystals (Si-nc-COOH) was obtained.

## 2.3. Dispersion of Si-nc in water and organic solvent

An aqueous suspension of Si-nc-COOH was obtained by re-suspending Si-nc-COOH ( $50 \text{ } \mu\text{l}$ ) in a volume of twice-distilled water ( $950 \text{ } \mu\text{l}$ , nominal  $15\text{--}18 \text{ M}\Omega \text{ cm}$  Millipore) and shaking for a few seconds. Aqueous solutions of Si-nc-COOH in the presence of surfactants were obtained by diluting Si-nc-COOH ( $50 \text{ } \mu\text{l}$ , ethanol suspension) in the aqueous solution ( $950 \text{ } \mu\text{l}$ ) containing 4-(2-hydroxyethyl)-1-piperazineethanesulfonic acid (HEPES, 10 mM) at pH 7.00 in the presence of sodium dodecyl (SDS, 10 mM) or of cetyl trimethylammonium bromide (CTAB, 1 mM).

## 2.4. Characterization

Time-resolved photoluminescence (TR-PL) measurements were performed using as an excitation source the third harmonic (355 nm, 6 ns pulse width, 10 Hz repetition rate) of a neodymium-doped yttrium aluminum garnet (Nd:YAG) laser with a photon flux of approximately  $10^{25} \text{ photons s}^{-1} \text{ cm}^{-2}$  on the sample. As a detection system, a CCD Streak camera interfaced with a spectrometer (10 ns of time resolution and 1 nm of spectral resolution) was used. Continuous wave photoluminescence (CW PL) measurements were done by a Cary Eclipse (Varian) fluorometer with an excitation wavelength of 350 nm. The quantum efficiency measurements

were performed using the 361 nm excitation line of a SpectraPhysics UV-extended argon ion laser. A Sopra monochromator interfaced with a visible photomultiplier tube (PMT) was used in detection (spectral resolution was 1 nm). The laser power was determined using an Ophir power meter calibrated at 365 nm. As a reference source a red LED (MV5052 produced by Fairchild Semiconductors) was used. The exact procedure is reported elsewhere [22]. All PL measurements were performed at room temperature and corrected for the spectral response of the detecting instruments. All solutions were contained in quartz cuvettes of 1 cm path length. The photo of Si-nc in figure 2(b) was taken by using a UV lamp as the excitation source.

## 3. Results and discussion

Si-nc are produced in a toluene/ethanol mixture (by sonication of just-etched porous silicon, see figure 1 and section 2 for additional info). Thus, as-prepared luminescent Si-nc are hydrophobic (hydrogen-terminated). Hence, it is necessary to modify their surface to a hydrophilic state to make them compatible with an aqueous environment. Although the surface modification into an hydrophilic state could be achieved by simply leaving the Si-nc immersed in water where oxidation slowly takes place [13], we prefer a more controlled approach. We used a photochemical hydrosilylation of the hydrogen-passivated Si-nc surface by undecylenic acid (see section 2) [23]. We call this process Si-nc functionalization. After functionalization, Si-nc are carboxylic-terminated (Si-nc-COOH) and they can be easily suspended both in ethanol and in water, producing luminescent suspensions (figure 2(b)). Conversely, the luminescence of non-functionalized Si-nc (Si-nc-H) is completely quenched in water (on a timescale where no significant oxidation occurs) and ethanol. We used this method instead of oxidation by water exposure for a number of reasons:

- carboxylic termination allows for straightforward coupling with different chemical and biological species [24];
- it is fast (modification of the surface lasts less than 2 h, see section 2);
- the process is controlled whilst water exposure is difficult to control [25];
- water exposure does not yield a stoichiometric oxide shell on the surface of the Si-nc. Suboxides are often formed which are related to efficient luminescence quenching centers [13].

The functionalized Si-nc were further characterized by means of transmission electron microscopy (TEM) and Fourier transform infrared spectroscopy (FTIR) confirming carboxyl capping of the produced nanocrystals (see supplementary data, figures S1 and S2 available at [stacks.iop.org/Nano/22/215704/mmedia](http://stacks.iop.org/Nano/22/215704/mmedia)).

Freshly prepared Si-nc-COOH suspended in ethanol show a broad red luminescence band (figure 2(a)), which peaks at around 640 nm and is 120 nm wide. The red photoluminescence is the first indicator that the PL we observe is due to quantum confinement effects (QCE) since the defect

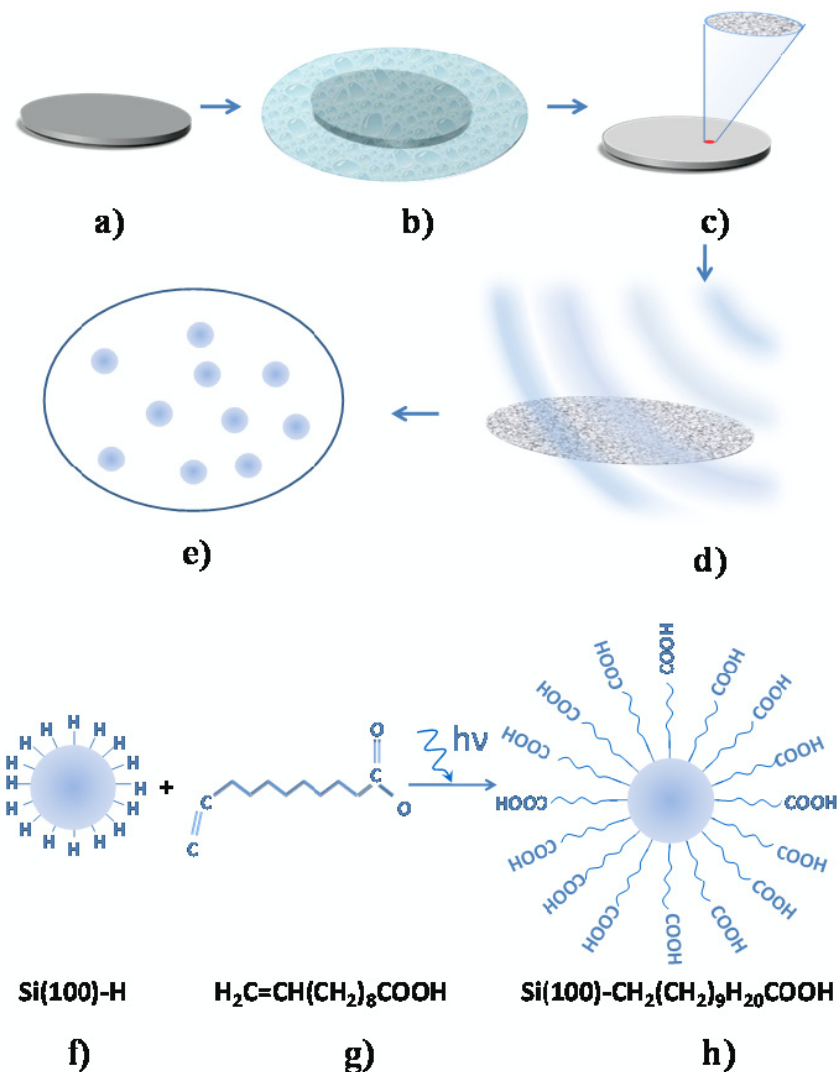


**Figure 1.** A silicon wafer (a) was electrochemically etched in HF/ethanol solution (b) to produce the porous silicon (c). Porous silicon was then sonicated (d) in toluene/ethanol solution to obtain Si-nc (e). The carboxyl-acid-terminated monolayer on the surface of the Si-nc-COOH (h) was achieved through the photochemical hydrosilylation of undecylenic acid (g) with a hydrogen-terminated Si(100) surface (f) of Si-nc (see section 2 for additional info).

band associated with oxide defects is usually in the blue [26]. The hydrosilylation is essential to produce a stable dispersion (figure 2(b)). The PL of such Si-nc-COOH is not quenched in ethanol [20] (figures 2(a) and (b)), further confirming that the surface of the particles is partially coated and, therefore, hardly accessible to dissolved species.

Once the Si-nc-COOH are suspended in water, their PL lineshape and peak position do not change with respect to what is observed for an ethanol suspension on short timescales (hours, figure 2(a)). Nevertheless, a rapid decrease of their PL intensity is observed immediately after suspension in water (figure 2(c)). This also points to a QCE nature of the emission, since emission due to interface states shows quite a different behavior when the nanocrystals are immersed in water [27]. The PL intensity decreases up to approximately 50% of its initial value in 10–15 min and then stabilizes (figure 2(c)). What is interesting is that, during the same time, the absorbance of the Si-nc-COOH suspension in water

increases rapidly and then stabilizes, too (figure 2(c)). The opposite trends between emission intensity and absorbance prove that these are not caused by a decrease of the Si-nc concentration (e.g. due to Si-nc precipitation).

In order to get some more insight into these phenomena and the origin of PL, TR PL measurements were performed on the Si-nc-COOH suspended in water after PL stabilization. As is commonly observed for Si-nc, the luminescence decay lineshape was a stretched exponential function [28]:

$$I(t) = I_0 \exp[-(t\tau^{-1})^\beta] \quad (1)$$

where  $I(t)$  is the PL intensity,  $\beta$  is the stretching parameter and  $\tau$  is a temporal parameter which for  $\beta = 1$  corresponds to the luminescence lifetime. The results of fitting the experimental data with the stretched exponential are reported in figure 2(d) (see also figure S4 in supplementary data available at [stacks.iop.org/Nano/22/215704/mmedia](http://stacks.iop.org/Nano/22/215704/mmedia)).

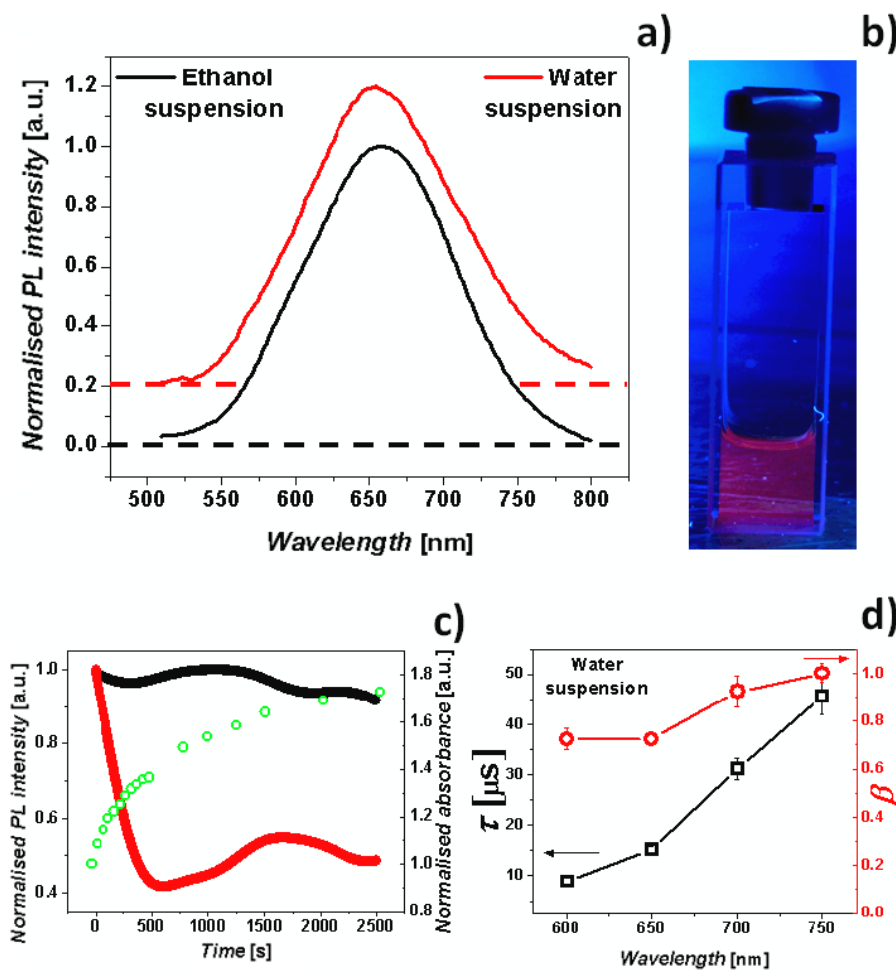


**Figure 2.** (a) Normalized PL spectra of functionalized Si-nc-COOH in ethanol (black line, down) and water (red line, up) suspension. PL spectra of functionalized Si-nc-COOH in water suspension is offset along the y axis by 0.2 for clarity, dashed line corresponding to zero. No visible spectral deformation could be observed for different suspensions. The excitation is at 361 nm. (b) Red photoluminescence from the Si-nc-COOH suspended in ethanol under illumination from UV lamp. (c) Time evolution of PL (full red circles) and absorbance (empty green circles) of functionalized Si-nc-COOH in water suspension upon UV excitation (361 nm). Both curves are normalized to the initial value of the PL intensity and of the absorbance, respectively. The long-term oscillations are due to a convective motion of heated solvent in the illuminated part, causing the small discrepancy in the dynamics of the PL and of the absorbance in the water suspension. To show this effect the PL evolution of Si-nc-COOH in ethanol suspension (black full circles) is also reported. (d) Stretched exponential fit parameters obtained from the fit of decay curves of functionalized Si-nc-COOH in water. Excitation is at 355 nm.

The time decay of the functionalized Si-nc-COOH was found to be in the microsecond range. Microsecond long lifetimes are compatible with the results of other studies where the emission is attributed to quantum confinement [18]. This is further confirmed by the strong wavelength dependence of the time decays (figure 2(d)). The observed trend is explained by the increase of the radiative rates as the Si-nc size decreases [18, 29]. This observation also implies a high crystalline quality of the Si-nc-COOH [30]. Furthermore, the high values of the dispersion parameter  $\beta$  (figure 2(d)) suggest that the Si-nc are isolated and no inter-dot hopping occurs [31]. The time decay of the functionalized Si-nc-COOH in water suspension is stable and it is not changing on short timescales (hours).

For Si-nc in ethanol suspension we find a quantum yield value of 30%, which agrees well with the values found in the literature on similar systems [32, 33], confirming a good

quality of produced Si-nc-COOH. From the quantum yield and the values for absorption cross section of Si-nc found in the literature [34], the concentration of functionalized Si-nc-COOH in ethanol suspension was estimated to be approximately  $10^{13}$  nc  $\text{cm}^{-3}$  (see supplementary data available at [stacks.iop.org/Nano/22/215704/mmedia](http://stacks.iop.org/Nano/22/215704/mmedia)). In the case of the Si-nc-COOH in water suspension, quantum yield measurements become unreliable (experimental error rises from 5% in ethanol suspension up to almost 20% for suspension in water) due to fluctuations of both the emission and the absorption (figure 2(c)). However, the data shown in figure 2(c) point to a quantum efficiency similar to that of the ethanoic suspension.

Let us try now to discuss the origin of the temporal dependence of the emission and absorption. The PL of Si-nc-COOH in ethanol suspension remains stable, even after long illumination (figure 2(c)). The initial fast temporal

decrease of the PL of Si-nc-COOH in water suspension does not depend on illumination. Indeed, experiments where the laser excitation was turned off and on demonstrate a decrease of the PL which was independent of the presence and the absence of the laser light, i.e. the decay continues even in the absence of illumination and the PL intensity is not recovered by turning off the illumination. Combining these observations with the unchanging PL lineshape and time decays, we can safely discard photobleaching (or light-stimulated surface chemical reactions) as the cause of the emission decrease of Si-nc-COOH in aqueous ambient. As well, a change in the dielectric constant of the surrounding medium between different suspensions (ethanol  $n = 1.36$  [35] and water  $n = 1.33$  [36] at  $\lambda = 640$  nm) is not enough to explain the considerable differences in PL and absorbance in these two solvents. Since the water and ethanol suspensions were produced by dissolution of the same amount of starting Si-nc-COOH, the concentration of the Si-nc-COOH in both suspensions is expected to be approximately the same. Thus, the increased absorbance in water suspension cannot be due to an increase of the electronic absorption of Si-nc-COOH (no PL lineshape change nor lifetime variations). The only possibility left is an increased scattering of light caused by the speeding-up of the agglomeration of Si-nc-COOH in water. We suggest the creation of small agglomerates of functionalized Si-nc-COOH in water due to polar repulsion as for micelle formation. In fact, the surface of Si-nc-COOH is only partially coated by the undecylenic acid [37]. Moreover, the functionalizing molecule introduces an alkyl chain, which imparts a partially hydrophobic character to the coated Si-nc-COOH. This yields small dynamic dominions of Si-nc-COOH in the strongly polar water. Since neither the suspension becomes opaque to an eye nor filtration over 200 nm filters changes the PL dynamic of the suspension and, moreover, the extinction saturates at values presented in figure 2(c), we expect the formation of relatively small agglomerates of Si-nc (sizes lower than 200 nm).

A qualitative estimate of this increased absorbance can be done by using the theory of Mie scattering of small scatterers [38]. In order to calculate the Mie scattering from the Si-nc-COOH, we did very crude approximations: a single size and spherical shape for the single isolated Si-nc-COOH and spherical large clusters of agglomerated compact Si-nc-COOH. The calculations were done with non-commercial software based on the classic Bohren and Huffman MIE (BHMIE) algorithm [39] for Mie scattering from a sphere in a medium [40]. For the medium, the refractive index of water at 25 °C and at the excitation wavelength was used. In the case of a wavelength scan, the refractive index of the medium was accordingly corrected. Since the refractive index of the Si-nc-COOH is not known (the literature reports only average refractive indices of the Si-nc embedded in a given matrix), we scan over a range of refractive indices which includes that of the bulk silicon at the suitable wavelength. Figure 3(a) shows the results of Mie scattering calculations where the absorbance (due to extinction)  $A_{\text{ext}}$  is reported at the wavelength of the excitation laser light. The absorbance is normalized to the value of Si-nc-COOH concentration (assuming a number density  $n_0 = 10^{13} \text{ cm}^{-3}$  and a particle diameter  $d_0 = 4$  nm

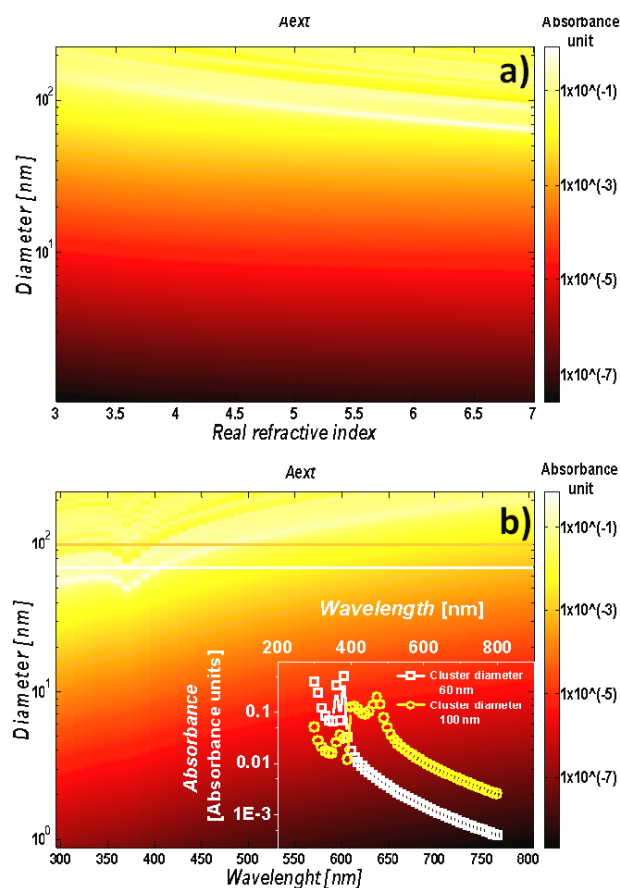


**Figure 3.** (a) Semi-log 2D maps of the absorbance due to scattering  $A_{\text{ext}}$  as a function of the real part of the refractive index ( $x$  axis) and Si-nc-COOH's cluster size ( $y$  axis). Wavelength of the incident light is fixed to 361 nm. The imaginary part of the refractive index is assumed to be zero. (b) Semi-log 2D maps of the absorbance due to scattering as a function of wavelength of the emitted light ( $x$  axis) and Si-nc-COOH's cluster size ( $y$  axis). Values and wavelength dependence of the real part of the refractive index of Si-nc-COOH are assumed to be the same as those of bulk silicon [42]. Imaginary part of the refractive index in both cases is assumed to be zero. Two horizontal lines represent cluster sizes for which semi-log plots have been generated (see inset). Inset: semi-log plot of the absorbance as a function of wavelength of the emitted light for two different cluster sizes with diameters 60 and 100 nm.

(which corresponds to the average size of Si-nc as deduced from the peak of PL)) which in our case scales as the inverse of the volume of the nanoparticle.

As can be observed from figure 3(a), there is a net increase of absorbance with increased Si-nc-COOH agglomerate size due to the increased scattering, for all the values of refractive index considered. The interference pattern observed at large cluster sizes and large refractive indices is due to the assumption of a monodisperse population of nanoparticles. As TEM imaging shows (see supplementary data available at [stacks.iop.org/Nano/22/215704/mmedia](http://stacks.iop.org/Nano/22/215704/mmedia)), we have a size distribution in the Si-nc-COOH which will eventually wash off the interference pattern without offsetting significantly the absorbance values found [41].

To infer whether the agglomeration affects also the intensity and lineshape of the emission we calculated the

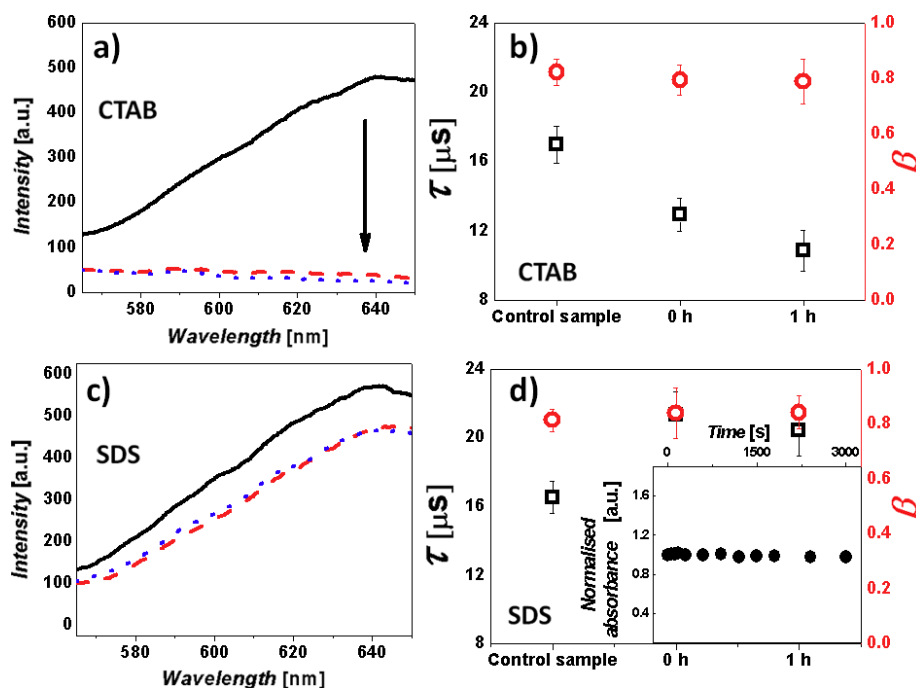


**Figure 4.** (a) PL spectra of functionalized Si-nc-COOH in water suspension (black solid line), immediately after adding the cationic surfactant CTAB (red dashed line) and one hour later (blue dotted line). Significant quenching of PL signal could be observed. (b) Stretched exponential fit parameters obtained from the fit of the 580–640 nm integrated decay curves of functionalized Si-nc-COOH in water suspension (control sample) and in water suspension with added cationic surfactant CTAB in different time intervals (immediately after adding and 1 h later). (c) PL spectra of functionalized Si-nc-COOH in water suspension (black solid line), immediately after adding the anionic surfactant SDS (red dashed line) and 1 h later (blue dotted line). (d) Stretched exponential fit parameters obtained from the fit of 580–640 nm integrated decay curves of functionalized Si-nc-COOH in water suspension (control sample) and in water suspension with added anionic surfactant SDS in different time intervals (immediately after, and after 1 h). Excitation is pulsed (6 ns, 10 Hz) and at 355 nm in all cases. Inset: time evolution of absorbance (full black circles) of functionalized Si-nc-COOH in water suspension with SDS in CMC. Curve is normalized to the initial value of absorbance. Note that, due to the streak camera used to measure the time decay and the time integrated spectra, the wavelength interval of the measurements is limited in figures 4(a) and (c).

spectral dependence of absorbance due to Mie scattering. The refractive index of bulk silicon at the absorption wavelength was assumed [42]. It can be seen from figure 3(b) that the computed absorbance is smaller than that found at the excitation wavelength. In addition, absorbance tends to decrease with the wavelength. It is interesting to note (inset to figure 3(b)) that the wavelength dependence of absorbance weakens with increased cluster size. The ratio of the absorbance value at the emission wavelength with respect to the value at the excitation wavelength increases from 0.3% for a 60 nm diameter cluster to 27% for a 100 nm diameter cluster. However, no PL quenching and spectral deformation of the PL band has been observed in the experiment, confirming that we are dealing with rather small aggregates. Aggregation has also been revealed by dynamic light scattering (DLS) experiments for the aqueous suspension of Si-nc-COOH, which gives typical cluster sizes of 120 nm. Small discrepancies with simulation are due to the approximations considered in the calculations.

If the ethanol Si-nc-COOH suspension is sonicated immediately before transferring to water, a smaller (than for a non-sonicated suspension) increase in the absorbance of the water suspension is observed ( $\sim 20\%$  more than in ethanol suspension). However, if the sonicated concentrated ethanol

suspension is left at rest for one week before the transfer to water, the absorbance shows the same trend as in figure 2(c). This implies that some agglomeration occurs also in ethanol, though to a lesser extent than in water. Aggregates in ethanol should be very small since absorbance does not change.

It is interesting to note that, despite agglomeration, the high value in the  $\beta$  coefficient measured by TR PL indicates that the nanocrystals are not interconnected in the aggregates.

To decrease the Si-nc-COOH agglomeration in water, we used surfactants. Two different surfactants were tested, which differ for their ionicity: sodium dodecyl (SDS—anionic) and cetyl trimethylammonium bromide (CTAB—cationic). They are representatives of the two different ionicity classes and have already been well characterized in the literature [43]. The control sample was an aqueous suspension.

In the presence of CTAB (1 ml, the critical micelle concentration (CMC)) [44], a significant blueshift and quenching of the emission is observed already after a few minutes (figure 4(a)). Concurrently, the lifetime decreases while the  $\beta$  parameter stays constant (figure 4(b)). These data can be interpreted as due to a quick hydroxylation and oxidation of Si-nc [43]. In the presence of SDS (7–10 mM, the CMC) [45], a slight decrease but no lineshape change are observed while the lifetime increases and the  $\beta$  parameter stays

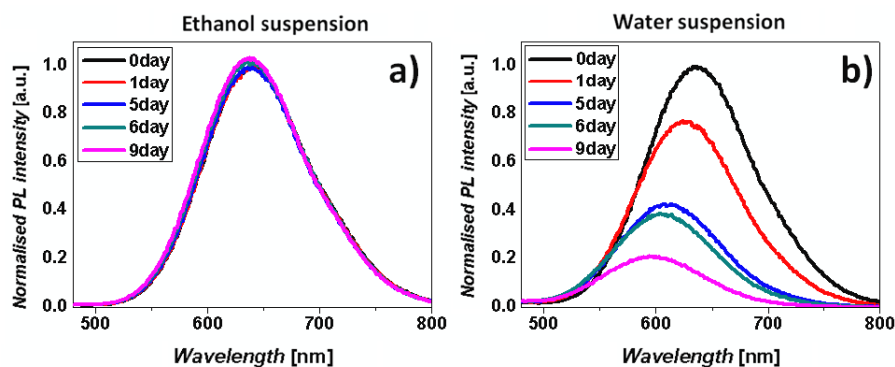


**Figure 5.** Time evolution of the PL of functionalized Si-nc-COOH on a long timescale (days) in different suspensions: (a) in ethanol suspension. PL is not quenched by ethanol and remains stable over a long time. (b) In water suspension. Blueshift of emission peak and decrease of PL intensity with time could be noticed. All spectra are normalized to the PL intensity of the zeroth day in their respective suspensions.

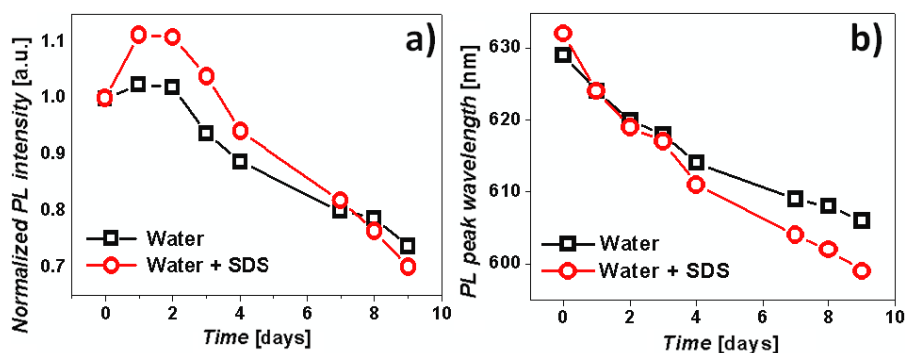


**Figure 6.** PL intensity (a) and peak wavelength (b) with time (days) of functionalized Si-nc-COOH in water suspension (black empty squares) and in water suspension with SDS added (10 mM, red empty circles). Excitation was at 350 nm. PL intensities are normalized to PL intensity of the zeroth day of the respective suspensions.

constant (figures 4(c) and (d)). The small decrease of the PL intensity can be due to the lengthening of the lifetime, i.e. to a decrease of the emission rate. It is important to notice that the absorbance of the suspension remains constant (figure 4 inset), indicating that no agglomeration occurs.

In the literature, there is no clear consensus on the mechanism and action of the anionic surfactant SDS, as there have been contradicting experimental reports [43, 46].

What becomes clear from our data is that SDS influences directly the PL lifetime of Si-nc-COOH. Since the lifetime is lengthened while the intensity is decreased, it looks that the overall effect is a lengthening of the radiative lifetime while the non-radiative lifetime is mostly unchanged. Thus, no further surface passivation occurs while most probably an electrostatic (Stark-like) separation in the electron-hole wavefunction causes the increase of the lifetime [47]. The electrostatic surface field might be due to the presence of the negatively charged group of adsorbed SDS molecules.

What we have discussed up to now is about the short timescale (hours). Figure 2 shows that, apart from the initial loss of intensity, the PL is stable both in intensity and color. This should allow us to use Si-nc-COOH as imaging probes, since their emission properties are maintained for a period

much longer than the typical renal clearance time for Si-nc of this size [48].

On a longer timescale (days), ethanol or aqueous suspensions behave differently (figure 5). Si-nc-COOH in ethanol remain stable while a constant blueshift in emission and a decrease in the emission intensity are observed for Si-nc-COOH in water. The same is also observed when SDS is added to the suspension (figure 6). This behavior is commonly attributed to a slow oxidation of Si-nc, which causes a decrease of the Si-nc-COOH core that is, in turn, reflected in a blueshift in the Si-nc-COOH emission [49]. In the case of interface PL activation during the oxidation in water, quite different behavior is observed [27]. The residual oxidation of the Si-nc-COOH is difficult to overcome by improving the degree of functionalization [37]. However, improved resistance to oxidation would most certainly decrease the biodegradability of such nanoparticles [13].

In particular, when SDS is added, a slight increase in the PL intensity after one day with respect to a bare aqueous suspension is observed (figure 6(a)). Moreover, the absorbance of the suspension with added SDS decreases while the aqueous solution maintains its values of absorbance from the previous day. This is caused by the lack of agglomeration with the

anionic surfactant. However, as the peak wavelength follows the same trend as the control samples (figure 6(b)) it is clear that SDS is not effective in increasing the degree of protection of Si-nc to the residual oxidation, nor interfering with the Si-nc-COOH biodegradability properties.

#### 4. Conclusions

We prepared highly luminescent Si-nc by sonication of porous silicon. Their solubility in polar solvents was achieved by surface functionalization with undecylenic acid through a light-driven hydrosilylation reaction. The obtained nanoparticles showed very stable PL characteristics in the ethanol suspension. Moreover, a high assembly quantum yield (~30%) was measured. However, the behavior of functionalized Si-nc-COOH was quite different in water suspension. In particular, we demonstrate that a limited agglomeration effect occurs on the nanoscale in ethanol and water suspensions, this effect being more pronounced in water. The increased scattering of such dynamic aggregates could interfere with optical measurements, causing the underestimate of Si-nc-COOH optical performance, particularly in quantum yield estimates. We found that exciton dynamics in water suspension is not influenced, implying that a high quantum yield of Si-nc (~30%) in water suspension is also achieved.

We propose as a driving mechanism to such behavior a partial surface functionalization. This allows a manifestation of weak hydrophilic character of functionalized Si-nc-COOH by dynamic aggregate creation. We also point out their dynamic nature as the aggregate size and presence is related to solvent type.

The effect of surfactants was also explored in light to decrease the agglomeration. Two different types of surfactants (cationic: CTAB and anionic: SDS) were employed. For CTAB we found a negative influence due to a rapid increase in the oxidation process, while SDS is shown to be effective in decreasing the agglomeration effects. In addition, we find that SDS influences directly the exciton dynamics by changing the radiative lifetime of Si-nc-COOH, causing a small net decrease in PL intensity on short timescales (hours).

On long timescales (days) the PL evolution of functionalized Si-nc-COOH in water suspension is dominated by slow Si-nc oxidation. On the other hand, the presence of SDS induces a net increase in PL intensity. We attribute it to a smaller degree of Si-nc-COOH's agglomeration in the presence of this surfactant. As well, SDS is not interfering with the oxidation process, maintaining the biodegradability of Si-nc-COOH.

#### Acknowledgments

The authors would like to thank Ramona Dallapiccola for the DLS measurements and Eveline Rigo for the photographs.

#### References

- [1] Amiot C L, Xu S, Liang S, Pan L and Zhao J X 2008 *Sensors* **8** 3082–105

- [2] O'Farrell N, Houlton A and Horrocks B R 2006 *Int. J. Nanomed.* **1** 451–72
- [3] Sengupta S, Eavarone D, Capila I, Zhao G, Watson N, Kiziltepe T and Sasisekharan R 2005 *Nature* **436** 568–72
- [4] Welsher K, Liu Z, Darancioglu D and Dai H 2008 *Nano Lett.* **8** 586–90
- [5] Kim D, Park S, Lee J H, Jeong Y Y and Jon S 2007 *J. Am. Chem. Soc.* **129** 7661–5
- [6] Voura E B, Jaiswal J K, Mattoussi H and Simon S M 2004 *Nat. Med.* **10** 993–98
- [7] Liu Z, Davis C, Cai W, He L, Chen X and Dai H 2008 *Proc. Natl Acad. Sci. USA* **105** 1410–5
- [8] Kirchner C, Liedl T, Kudera S, Pellegrino T, Javier A M, Gaub H E, Stolzle S, Fertig N and Parak W J 2005 *Nano Lett.* **5** 331–8
- [9] Green M and Howman E 2005 *Chem. Commun.* **1** 121–23
- [10] Poland C A, Duffin R, Kinloch I, Maynard A, Wallace W A H, Seaton A, Stone V, Brown S, MacNee W and Donaldson K 2008 *Nat. Nanotechnol.* **3** 423–28
- [11] Popplewell J F, King S J, Day J P, Ackrill P, Fifield L K, Cresswell R G, Tada M L and Liu K 1998 *J. Inorg. Biochem.* **69** 177–80
- [12] Bayllis S C, Heald R, Fletcher D I and Buckberry L D 1999 *Adv. Mater.* **11** 318–21
- [13] Park J H, Guo L, Maltzahn G, Ruoslahti E, Bhatia S N and Sailor M J 2009 *Nat. Mater.* **8** 331–6
- [14] Frangioni J V 2003 *Curr. Opin. Chem. Biol.* **7** 626–34
- [15] Benson R C and Kues H A 1978 *Phys. Med. Biol.* **23** 159–63
- [16] Canham L T 1990 *Appl. Phys. Lett.* **57** 850–2
- [17] Yuan Z, Anopchenko O, Daldosso N, Guider R, Navarro-Urrios D, Pitanti A, Spano R and Pavesi L 2009 *Proc. IEEE* **97** 1250–68
- [18] Hybertsen M S 1993 *Phys. Rev. Lett.* **72** 1514–8
- [19] Godefroo S, Hayne M, Jivanscu M, Stesmans A, Zacharias M, Lebedev O I, Van Tendeloo G and Moshchalkov V V 2008 *Nat. Nanotechnol.* **3** 174–8
- [20] Sailor M J and Wu E C 2009 *Adv. Funct. Mater.* **19** 3195–208
- [21] Veinot J G C 2006 *Chem. Commun.* **42** 4160–8
- [22] Karakuscua A, Guider R, Pavesi L and Sorarù G D *Thin Solid Films* **519** 3822–6
- [23] Erogbogbo F, Yong K T, Roy I, Xu G, Prasad P N and Swihart M T 2008 *ACS Nano* **2** 873–8
- [24] Li Z F, Kang E T, Neoh K G and Tan K L 1998 *Biomaterials* **19** 45–53
- [25] Kang Z, Liu Y, Tsang C H A, Ma D D D, Fan X, Wong N B and Lee S T 2009 *Adv. Mater.* **21** 661–4
- [26] Fauchet P M 1996 *J. Lumin.* **70** 294–309
- [27] Gupta A and Wiggers H 2011 *Nanotechnology* **22** 055707
- [28] Lindsey C P and Patterson G D 1980 *J. Chem. Phys.* **73** 3348–57
- [29] Takagahara T and Takeda K 1992 *Phys. Rev. B* **46** 15578–81
- [30] Fujii M, Imakita K, Watanabe K and Hayashi S 2004 *J. Appl. Phys.* **95** 272–80
- [31] Pavesi L and Ceschini M 1993 *Phys. Rev. B* **48** 17625–28
- [32] Credo G M, Mason M D and Buratto S K 1999 *Appl. Phys. Lett.* **74** 1978–80
- [33] Jurbergs D, Rogojina E, Mangolini L and Kortshagen U 2006 *Appl. Phys. Lett.* **88** 233116
- [34] Kovalev D, Diener J, Heckler H, Polisski G, Kunzner N and Koch F 2000 *Phys. Rev. B* **61** 4485–7
- [35] Rheims J, Koser J and Wriedt T 1997 *Meas. Sci. Technol.* **8** 601–5
- [36] Hale G M and Query M R 1973 *Appl. Opt.* **12** 555–63
- [37] Sieval A B, Van Den Hout B, Zuillhof H and Sudhölter E J R 2001 *Langmuir* **17** 1457–60
- [38] Mie G 1908 *Ann. Phys.* **330** 377–445
- [39] Bohren C F and Huffman D R 1983 *Absorption and Scattering of Light by Small Particles* (New York: Wiley) p 541

- [40] Philip L *MiePlot* <http://www.philiplaven.com>
- [41] Mishchenko M I, Travis L D and Lacis A A 2002 *Scattering, Absorption and Emission of Light by Small Particles* (Cambridge: Cambridge University Press) p 445
- [42] Green M A and Keevers M J 1995 *Prog. Photovolt.* **3** 189–92
- [43] Canaria C A, Huang M, Cho Y, Heinrich J L, Lee L I, Shane M J, Smith R C, Sailor M J and Miskelly G M 2002 *Adv. Funct. Mater.* **12** 495–500
- [44] Pagac E S, Prieve D C and Tilton R D 1998 *Langmuir* **14** 2333–42
- [45] Fuguet E, Ràfols C, Rosés M and Bosch E 2005 *Anal. Chim. Acta* **548** 95–100
- [46] Chattopadhyay S and Bohn P W 2006 *Anal. Chem.* **78** 6058–64
- [47] Kulakci M, Serincan U, Turan R and Finstad T G 2008 *Nanotechnology* **19** 455403
- [48] Choi H S, Liu W, Misra P, Tanaka E, Zimmer J P and Ipe B I 2007 *Nat. Nanotechnol.* **25** 1165–70
- [49] Chirvony V, Chyryonaya A, Ovejero J, Matveeva E, Goller B, Kovalev D, Huygens A and De Witte P 2007 *Adv. Mater.* **19** 2967–72